JOURNAL OF MATERIALS SCIENCE 8 (1973) 1123–1125

The thermal expansion of single-crystal texture linear polyethylene between 0 and −190°C

C. P. BUCKLEY*, N. G. McCRUM
Department of Engineering Science, Oxford University, UK

Thermal expansion of linear polyethylene in both macroscopically isotropic and single-crystal texture forms was measured between 0 and − 190°C. Results are interpreted by treating the semicrystalline polymer as a simple two-phase composite material. The single-crystal texture specimen was prepared by drawing with constant width at 121°C followed by annealing, giving unique preferred orientations of each of the three crystal axes *a*, *b* and *c* (*c* parallel to the draw direction *Z*, *a* parallel to the sheet normal *X* and *b* parallel to *Y*, the normal to the thin edge of the sheet). The thermal expansions parallel to *X*, *Y* and *Z* follow approximately the thermal expansions of *a*, *b* and *c* vectors of the unit cell as determined by X-ray diffraction. An attempt is made to allow for the contribution to thermal expansion from amorphous regions, representing the oriented solid by a simple model in which crystal and amorphous regions are coupled in series in the draw direction and in parallel in the two perpendicular directions. This analysis requires the thermal expansion of amorphous polyethylene which was obtained by extrapolation of thermal expansion measurements on ten isotropic specimens whose crystal volume fractions lay between 0.81 and 0.49. It was observed that the single crystal texture specimen of crystal fraction 0.80 and an isotropic specimen of the same crystal fraction on cooling changed in volume by equal amounts. This fact together with the observation that the thermal expansion parallel to *Y* of the single crystal texture specimen is equal to that of the isotropic specimen leads to important conclusions concerning the existence of microstresses in linear polyethylene caused by a change of temperature.

1. Introduction

Anisotropy of the tensile compliance of oriented crystalline polymers is known to be dominated by the mode of coupling between crystalline and amorphous regions. Thus, for tensile stress parallel to the draw direction there is approximately series coupling while perpendicular to the draw direction there is parallel coupling [1-4]. These considerations have led to model calculations of the compliance of oriented linear polyethylene (LPE) in terms of: 1. the known texture of the oriented solid (distribution of crystal axes); 2. the anisotropic moduli of the crystal and the modulus of the amorphous fraction; 3. the volume fraction of the two phases. The fit to experiment based on the elementary Takayanagi model as applied to oriented polymers [2] has been fair [3, 4]. If the Takayanagi model has validity there is every reason to expect it also to predict the anisotropic thermal expansion of oriented LPE. This was the major purpose of the experiments described in this paper.

It is our purpose to compare the measured expansivities of a specimen of LPE oriented with *a*, *b* and *c* crystal axes along the three co-ordinate axes of the specimen with the predictions of a simple Takayanagi model. In brief the experiment consists of:

1. preparing a sheet of LPE oriented with single crystal texture so that the crystalline *a*, *b* and *c* axes lie in preferred directions along *X*, *Y* and *Z* directions of the specimen as indicated in Fig. 1;
2. obtaining pole figures for *a*, *b* and *c* poles and

*Present address Centre de Recherches sur les Macromolécules, 6 Rue Boussingault, 67 Strasbourg, France.

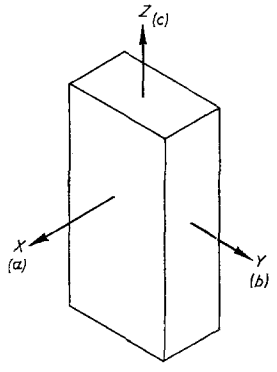

Figure 1 Co-ordinates of specimen showing direction of preferred alignment of crystal axes. Specimen formed by drawing parallel to Z, and constrained in the Y direction. Measured distribution of crystal axes around XYZ shown

observing the distribution of lamellar normals by small-angle X-ray diffraction;
3. measuring the thermal strains from 0 to − 190°C of the biaxially oriented solid along X, Y and Z directions (we were in practice not able to obtain measurements in the X direction below − 120°C);
4. measuring the thermal strains for amorphous polyethylene from 0 to − 190°C using the extrapolation method of Stehling and Mandelkern [5];
5. using the latter values and the crystal thermal strain values of Davies, Eby and Colson [6] to calculate from the model the predicted thermal strains for the biaxially oriented solid in the X, Y and Z directions.

2. Review of thermal expansion measurements on LPE

The aim of the present work is to bring together knowledge of the thermal expansions of crystalline and amorphous regions of LPE, in order to predict the anisotropic thermal expansion of oriented LPE. It is expedient to first briefly review existing knowledge of thermal expansion in crystal and amorphous phases of this polymer.

2.1. Measurements by X-ray diffraction

For any solid containing crystals, the method of wide-angle X-ray diffraction may be used to measure the variation with temperature of the distances between lattice planes. For a crystal of orthorhombic symmetry, such as that of polyethylene, this yields directly the anisotropic linear thermal expansion of the lattice in different crystallographic directions. The technique has been applied to polyethylene to measure the linear thermal expansion of the crystal in directions a, b and c.

It is now well established that thermal expansion of the polyethylene crystal unit cell occurs largely through expansion in the a direction. Several studies have shown the coefficient of linear thermal expansion in the a direction, α_a, to greatly exceed that in the b direction, α_b, at all temperatures so far covered [6-14]. Probably the most precise data available are those of Davis *et al* [6] which yield $\alpha_a = 3.1 \times 10^{-4}°C^{-1}$ and $\alpha_b = 0.7 \times 10^{-4}°C^{-1}$ at room temperature. The difference between α_a and α_b is believed to reflect the predominance of chain rotation in the vibrational spectrum of the polymer crystal. Several authors have pointed out that if the ratio $a:b$ reached $\sqrt{3}$ then the crystal would show a transition to hexagonal symmetry [7, 13, 14]. In practice even at the melting point this ratio achieves a value of only 1.56 in LPE [3] and consequently polyethylene exhibits no such transition.

Some authors have reported a sharp increase in α_a in the temperature range 50 to 100°C [10, 12, 14], perhaps corresponding to the crystal relaxation observed by dielectric and NMR techniques in this temperature region. This feature, however, does not occur consistently and did not appear in other studies which covered the same temperature range [7-9, 13]. Recent evidence suggests that the precise values of a and α_a, particularly at room temperature and above, depend upon crystallization conditions [6].

Thermal expansion parallel to the c-axis is more difficult to measure, both because of the low intensity of the (002) X-ray reflection in polyethylene, and because α_c differs little from zero. It has been known for some time, however, that a wide range of other polymer crystals exhibit a negative linear thermal expansion coefficient parallel to the chain axis [11]. This was found to be the case for polyethylene by Cole and Holmes [9], who obtained $\alpha_c = -0.52 \times 10^{-4}°C^{-1}$, although this variation of c was close to the limit of their experimental error. Swan [13] also could not reliably distinguish α_c from zero, when taking experimental error into account. Improvement in technique has enabled more recent studies to clearly resolve a negative value for α_c. Kobayashi and Keller [15] obtained $\alpha_c = -0.12 \times 10^{-4}°C^{-1}$ close to room temperature, while the data of Davis *et al* [6] affords an

average value of $\alpha_c = -0.13 \times 10^{-4}°C^{-1}$ (for the 2.5 h specimen of their paper). It may now be considered established that α_c is indeed negative. This may be simply explained on the basis of increased amplitude of rotational oscillation around the C-C bond occurring with increase in temperature [6, 15].

Wide-angle X-ray diffraction has also been used to measure thermal expansion of amorphous regions of polyethylene, by taking the spacing of the amorphous "halo" to represent an average spacing between molecules in these regions. A serious drawback to this method is the doubt that exists over the correct molecular interpretation of this spacing. Applying the technique to branched polyethylene (BPE), Ohlberg and Fenstermaker [16] obtained a sharp change in thermal expansion coefficient at a temperature of $-28°C$, suggesting that this is the glass transition temperature, T_g, for BPE. Sella [8] and Zalwert [14] have made measurements in this way on LPE above room temperature. Both authors found a sharp increase in thermal expansion coefficient in the range 50 to 100°C. It may be associated with an amorphous contribution to the mechanical α-relaxation which occurs in this temperature region [17].

A novel approach to the subject of thermal expansion in crystalline polymers has recently been adopted by Fischer and co-workers [18]. These authors measured the intensity of small angle X-ray scattering as a function of temperature, in this way obtaining the difference $\rho_{am}\beta_{am} - \rho_{cr}\beta_{cr}$, where β is the coefficient of volumetric thermal expansion, ρ is the density and subscripts am and cr refer to amorphous and crystalline regions respectively. The method was applied to single crystal mats of polyethylene, both linear and branched [18]. The results clearly indicated two regions along the temperature, T, axis. At low temperatures, $T < -26°C$ (BPE) or $T < -125°C$ (LPE) $\rho_{am}\beta_{am} - \rho_{cr}\beta_{cr} = 0$. Above these temperatures $\rho_{am}\beta_{am} - \rho_{cr}\beta_{cr} = 4.2 \times 10^{-4}$ g cm^{-3} °C^{-1} for BPE and $\rho_{am}\beta_{am} - \rho_{cr}\beta_{cr} = 3.9 \times 10^{-4}$ g cm^{-3}°C^{-1} for LPE. From the sharp distinction between these two regimes the authors concluded that -26 and $-125°C$ correspond to T_g for BPE and LPE, respectively [18]. The results are, therefore, in agreement with the amorphous "halo" measurements of Ohlberg and Fenstermaker for BPE [16] and the recent dilatometric work of Stehling and Mandelkern for LPE [5].

2.2. Measurement by dilatometry

Several dilatometric studies have aimed at measuring T_g for amorphous polyethylene. In practice, T_g was identified as the temperature at which there was a sharp change in slope of the specific volume (V_{sp}) versus T curve [19-22], or at which the coefficient of thermal expansion (linear or volumetric) became independent of degree of crystallinity [21, 23]. Danusso *et al* [19], Gubler and Kovacs [21] and Tanaka [22] have found T_g ,when measured in this way, to lie in the range -20 to $-25°C$ for both LPE and BPE. Nakane [23], however, obtained $T_g = -55°C$ and Dannis [20] $T_g = -122°C$ for LPE. The reason for this wide discrepancy lies in the shape of the V_{sp} versus T curve for a highly crystalline polymer such as LPE which strongly reflects the thermal expansion of the crystals. The "knee" in the curve, used to obtain T_g, is, therefore, ill-defined. This problem was acknowledged by Quinn and Mandelkern [24], who emphasised the need for dilatometric data to cover a wide temperature range. When data for LPE covers a range from $-180°C$ to room temperature, the most pronounced "knee" is clearly seen to occur at about $-125°C$ [20, 24]. This volumetric transition is termed γ-transition since it is clearly associated with the mechanical γ-relaxation ($-127°C$, 0.67 Hz).

Convincing evidence that the γ-transition is the glass transition of amorphous LPE has been provided by the recent dilatometric study by Stehling and Mandelkern [5]. These authors measured the linear thermal expansion of isotropic samples of LPE encompassing a wide range of crystallinity. Extrapolation of the coefficient of linear thermal expansion to zero crystallinity gave that value corresponding to amorphous LPE. This was found to undergo an abrupt change in the range $T = -133 \pm 7°C$, exhibiting values above and below this region similar to those of wholly amorphous polymers above and below T_g. This work supports therefore the earlier work of Dannis [20] and calls for reappraisal of the results of Danusso *et al* [19], Gubler and Kovacs [21], Tanaka [22] and Nakane [23].

3. Experimental

3.1. Specimen preparation

A quenched compression moulded plate of Rigidex 2 (BP Chemicals Ltd) was drawn at 121°C in air. The sheet width was maintained nearly constant during drawing, and a uniform

draw ratio of 9 was achieved within the necked region. The resulting transparent sheet was then annealed at 127°C for 1 h, after which it was still transparent and of density $\rho = 0.971$ g cm^{-3} at 23°C. Wide-angle X-ray pole figures for (200), (020) and (002) poles are shown in Fig. 2. It will be seen that the *a*-, *b*- and *c*-axes are closely distributed about the *X*, *Y* and *Z* axes of the specimen.

The specimen is of course polycrystalline being composed of crystalline lamellae separated by amorphous polyethylene. The term single-crystal texture is used to describe the close distribution of *a*-, *b*- and *c*-axes around *X*, *Y* and *Z*. Small-angle X-ray scattering patterns showed the lamellar normals to be closely distributed about the *Z*-axis. A greater population of lamellar normals was observed in the *XZ* plane than in the *YZ* plane.

Plastic deformation of any semicrystalline polymer causes crystalline regions to be broken into smaller units containing an enhanced concentration of crystal defects, and amorphous regions to suffer molecular alignment. Recent work, however (see, for example, Fischer *et al* [25]), has shown that annealing of drawn LPE at temperatures approaching 130°C leads to relaxation of both types of region, which then become indistinguishable from their counterparts in undrawn LPE. In the following, this will be assumed to be the case for the present oriented specimens.

Isotropic specimens of linear polyethylene were prepared by moulding sheets of Rigidex 2 (BP Chemicals Ltd) and Hifax 1900 (Hercules Incorporated). They were each subjected to different heat-treatments in order to obtain ten specimens covering a wide range of crystallinity. The six specimens of Rigidex 2 studied here were the same as those of a previous study of low temperature properties of LPE [26]. The availability of Hifax 1900 high molecular weight LPE enabled the crystallinity range to be considerably extended in the present work. Four specimens of Hifax 1900 were prepared.

A sheet of Hifax 1900, 0.15 cm thick (machined from the centre of the $\frac{1}{4}$ in thick as-received sheet) was heated to 160°C under light pressure and then quenched into iced water. It was re-machined to a thickness of 0.10 cm, by removing 0.025 cm from each face. A portion of this sheet was annealed at 113°C for 2.5 h and slow cooled. A second 0.15 cm thick sheet of Hifax 1900 was heated in a similar fashion to 160°C but was then slow cooled at a rate of 2°C min^{-1}. This was also re-machined to a thickness of 0.10 cm. A portion was annealed at 118°C for 2.5 h and slow cooled.

The heat-treatments of the series of specimens are summarized in Table I, together with the corresponding sample densities measured at 23°C, ρ (23), and volume fraction crystallinities χ_v (calculated from ρ (23), taking ρ_{am} (23) = 0.853 g cm^{-3} and ρ_{cr} (23) = 1.000 g cm^{-3} [27]). The lower limit on χ_v has been reduced to 0.494 by use of the Hifax 1900 specimens.

3.2. Thermal expansion measurements

Let l_T and l_0 be the free specimen length at T°C and 0°C; similarly let V_T and V_0 be the free specimen volume at temperatures T°C and 0°C. Then, if the specimen temperature changes from 0 to T°C, we may define the linear thermal strain (expansivity) e and volumetric thermal strain

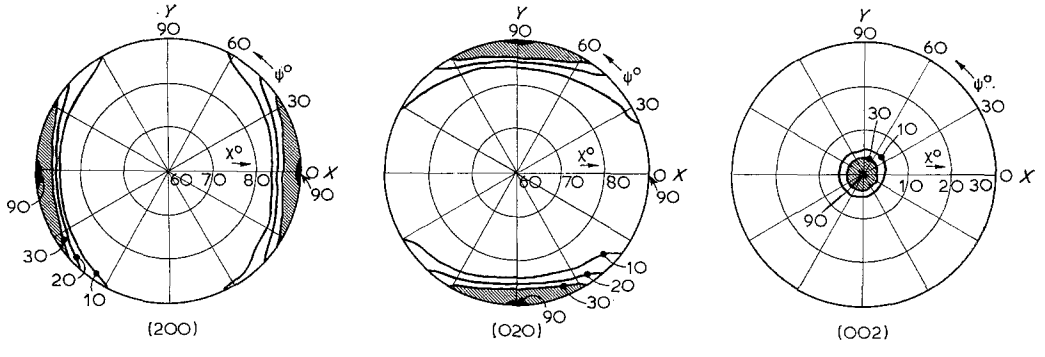

Figure 2 Pole figures for (200), (020) and (002) poles: shown as polar plots centred on the *Z* axis, in terms of polar angles ψ and χ. Only part of the scattering hemisphere is shown in each case. Contours indicated are percentages of peak intensity.

TABLE I Description of isotropic specimens including polymer type, moulding and annealing conditions, density at 23°C and crystal volume fraction χ_v.

Polymer	Moulding conditions	Heat-treatment	Density ρ (23) g cm^{-3}	χ_v
Hifax 1900	Quenched from melt into iced water	None	0.926	0.494
	as above	2.5 h at 113°C	0.930	0.520
	Cooled from melt at 2°C min^{-1}	None	0.937	0.571
	as above	2.5 h at 118°C	0.938	0.579
Rigidex 2	Quenched from melt into iced water	None	0.952	0.673
	as above	0.5 h at 111°C	0.958	0.714
	Cooled from melt at 13°C min^{-1}	None	0.963	0.748
	as above	5 h at 120°C	0.967	0.775
	Cooled from melt at 0.5°C min^{-1}	None	0.970	0.794
	as above	10 h at 120°C	0.972	0.808

(expansivity) e_v, which occur as a result of thermal expansion:

$$e \equiv \frac{l_T - l_0}{l_0} \tag{1}$$

$$e_v \equiv \frac{V_T - V_0}{V_0} . \tag{2}$$

For an isotropic solid e and e_v are related through

$$1 + e_v = (1 + e)^3 . \tag{3}$$

For many materials over a moderate range of temperature T, Equation 3 may be approximated, to a high degree of accuracy, by

$$e_v \simeq 3e . \tag{4}$$

Equation 4 cannot be applied, however, to polymeric solids for a temperature increment of 100°C or more, since errors of 1% or greater would be incurred. In this case the approximation

$$e_v \simeq 3e(1 + e) \tag{5}$$

is appropriate, with an error of only about 0.01%. The coefficients of linear thermal expansion, α, and of volumetric thermal expansion, β, are defined in terms of l_T and V_T thus

$$\alpha \equiv \frac{1}{l_T}\frac{\partial l_T}{\partial T} \tag{6}$$

$$\beta \equiv \frac{1}{V_T}\frac{\partial V_T}{\partial T} . \tag{7}$$

They are, therefore, related to the thermal strains e and e_v as follows:

$$\alpha = \frac{1}{(1 + e)}\frac{\partial e}{\partial T} \tag{8}$$

$$\beta = \frac{1}{(1 + e_v)}\frac{\partial e_v}{\partial T} \tag{9}$$

For an isotropic solid they are related themselves, through

$$\beta = 3\alpha . \tag{10}$$

It should be noted that for a polymer such as polyethylene, α and β are strong functions of temperature, i.e., curves of e or e_v versus T show much curvature. Precision of measurement of α or β is therefore usually poor, even though e and e_v might be known to acceptable precision. For this reason results will be presented here as e or e_v.

The biaxially oriented sample of LPE studied in this work possesses orthorhombic symmetry with principal axes X, Y and Z. The axes X, Y and Z are the principal axes of thermal strain. Thermal expansion of such a sample is completely specified by the three linear thermal strains, e (Equation 1) when l is measured parallel to X-, Y- and Z-axes. Let these be denoted by e_x, e_y, e_z respectively. The volumetric thermal strain e_v, again given by Equation 2, is exactly related to e_x, e_y and e_z through

$$1 + e_v = (1 + e_x)(1 + e_y)(1 + e_z) . \tag{11}$$

For many materials, Equation 11 would be adequately approximated by

$$e_v \simeq e_x + e_y + e_z . \tag{12}$$

In the present case, however, the following form is appropriate, with an error of less than 0.1%:

$$e_v \simeq e_x(1 + e_y) + e_y + e_z . \tag{13}$$

By analogy to the isotropic case, we may calculate the coefficients of linear thermal expansion measured in X, Y and Z directions α_x, α_y and α_z. In terms of e_x, e_y and e_z these are given by

$$\alpha_x = \frac{1}{(1 + e_x)}\frac{\partial e_x}{\partial T} , \quad \alpha_y = \frac{1}{(1 + e_y)}\frac{\partial e_y}{\partial T} ,$$

$$\alpha_z = \frac{1}{(1 + e_z)}\frac{\partial e_z}{\partial T} . \tag{14}$$

The analogous equation to Equation 10 is

$$\beta = \alpha_x + \alpha_y + \alpha_z . \quad (15)$$

For the isotropic polymer, e_v was determined by measuring e (Equation 5). This was performed by observing the change in length of a specimen as the temperature was raised from near liquid nitrogen temperature to 0°C at an average rate of 15°C h^{-1}. The initial cooling to liquid nitrogen temperature was performed slowly over a period of about 6 h. The specimen (a blade of size 0.1 cm × 0.3 cm × 3.5 cm) was clamped at both ends and maintained in a vertical position with an extremely small positive tension (approximately 3×10^5 dyn cm^{-2}). The change in length was observed by means of a calibrated linear differential transformer. With this technique the error in measured values of e was estimated to be never greater than $\pm 4\%$, and for temperatures below − 30°C less than $\pm 2\%$. Temperature variation along the specimen length never exceeded 1°C. The same apparatus was used to determine for the oriented polymer e_y and e_z from measurements in the plane of the plate. For the oriented polymer e_v was determined by the method of Sauer *et al* [28] using ethanol as the liquid. By using Equation 13, e_x was calculated from e_y, e_z and e_v [note e_x was difficult to determine by linear measurements normal to the plane of the plate since the specimen was extremely thin (0.1 cm)].

4. Results

4.1. Oriented specimen

The results for oriented LPE are shown in Fig. 3. The greater degree of experimental scatter in e_x, as compared with e_y and e_z, arises from the greater scatter in e_v which is used to compute e_x from Equation 13.

The reader will have anticipated that thermal expansions in the X, Y, Z directions of the sheet should follow approximately the expansions of the crystal in the a, b and c crystallographic directions. That this is indeed so may be seen by comparing the measured values of e_x, e_y and e_z shown in Fig. 3 with values of e_a, e_b and e_c shown in Fig. 4 [the latter being determined by X-ray diffraction by Davis *et al*, 2.5 h specimen]. This fact will be discussed in detail below.

If X, Y and Z are principal axes of thermal strain for these specimens, the linear thermal strain $e(\theta)$ measured in the YZ plane at an angle $\theta°$ to Z should be given by (noting that in the present case thermal strains cannot be considered infinitesimal)

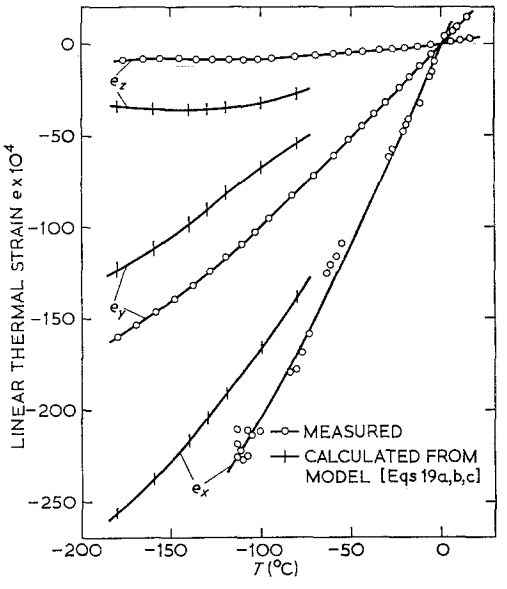

Figure 3 Linear thermal strains parallel to X, Y and Z axes plotted against temperature T: measured values (o) compared with predictions of model (Equations 19a, b and c).

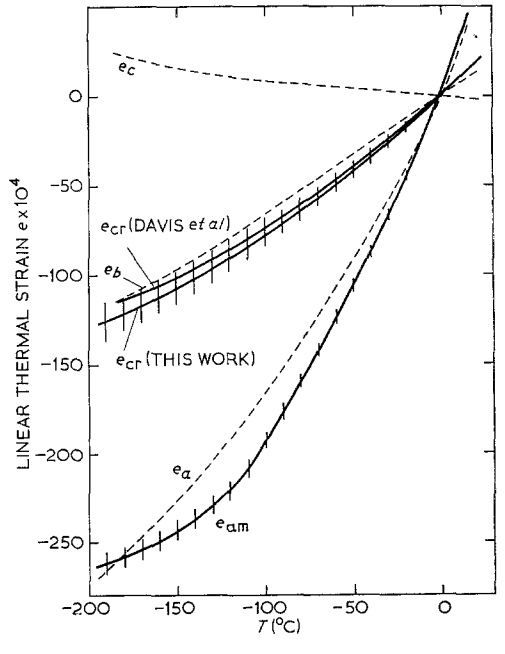

Figure 4 Temperature dependence of e_a, e_b and e_c (determined by X-ray diffraction [6]) compared with temperature dependence of e_{am} and e_{cr}.

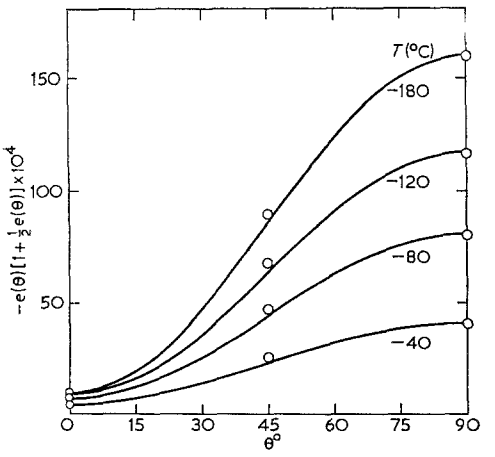

Figure 5 Angular dependence of linear thermal strain in the *YZ* plane: experimental values o; full curves calculated from Equation 16 using experimental values determined at 0 and 90°.

$$e(\theta_0)\,[1 + \tfrac{1}{2}e(\theta_0)] = e_y[1 + \tfrac{1}{2}e_y]\sin^2\theta_0 + e_z[1 + \tfrac{1}{2}e_z]\cos^2\theta_0\,, \quad (16)$$

where θ_0 is the value of θ at 0°C, when e is defined by Equation 1. The complete angular dependence of $e(\theta)$ in the *YZ* plane is, therefore, known if e_y and e_z have been measured.

For the oriented sheet studied here, e (45) was measured in addition to e_y and e_z. In Fig. 5 the function $e(\theta_0)\,[1 + \frac{1}{2}e(\theta_0)]$ calculated from e_y and e_z is shown for four values of temperature T. Also shown are the measured values of e (45) $[1 + \frac{1}{2}e\,(45)]$. These values lie on the theoretical curve to within about 3×10^{-4}, a small deviation which could be caused by an error in θ_0 of only 2°.

4.2. Isotropic specimens

The measured linear thermal strain e is shown as a function of temperature in Fig. 6 for five representatve isotropic specimens. All curves pass through the origin, from the definition of e in Equation 1. The prominent feature of the results is a systematic increase in magnitude of e with decreasing crystallinity χ_v, for any given temperature T. This simply reflects the greater thermal expansion of amorphous LPE as compared with crystalline LPE. In general features the results of Fig. 6 resemble the data of Stehling and Mandelkern [5].

Our purpose here is to obtain that value of e corresponding to amorphous LPE, e_{am}. How may this be achieved, given the complex morphology of isotropic semicrystalline LPE? Assume the polymer solid to be an isotropic two-

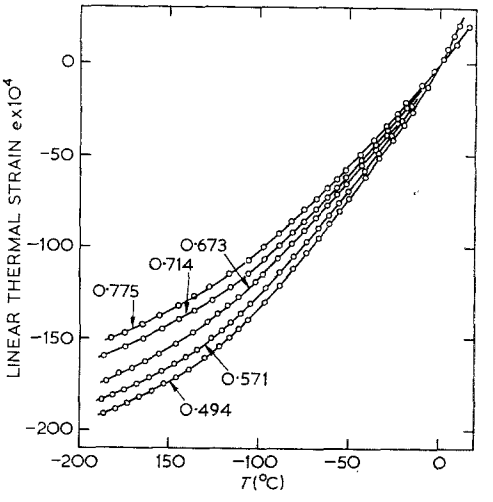

Figure 6 Temperature dependence of linear thermal strain for isotropic specimens of LPE with various volume fraction crystallinities χ_v.

phase composite material containing isotropic phases of arbitrary phase geometry. Several equations have been proposed for predicting the value of e for such a system. They are summarized in the Appendix. Let subscripts 1 and 2 denote the individual phases, and take $e_1 = -250 \times 10^{-4}$, $e_2 = -125 \times 10^{-4}$, $\nu_1 = 0.4$, $\nu_2 = 0.3$ and $G_2 = 5G_1$, where the elastic properties of each phase are defined by Poisson's ratio, ν, and shear modulus, G. With these values for the respective phase properties, the various predictions for e are plotted versus v_2, the volume fraction of phase 2, in Fig. 7. Neglecting Turner's equation (A2) which has not found wide application to polymeric systems [29, 30] the difference between the various predictions never exceeds about 5%.

Now the values assigned above to the phase properties correspond approximately to those of the two phases of LPE, for a temperature $T = -160$°C (with 1 corresponding to the amorphous phase and 2 to the crystals). From Fig. 7, therefore, a simple linear relationship between e and v_2 may be assumed, to a good approximation. Applied to the present problem this becomes

$$e = \chi_v e_{cr} + (1 - \chi_v)e_{am} \quad (17)$$

where e_{cr} is the linear thermal strain of the (assumed) isotropic crystal. The characteristic feature of Equation 17 is the assumption that thermal stresses are everywhere zero.

Further support for the application of

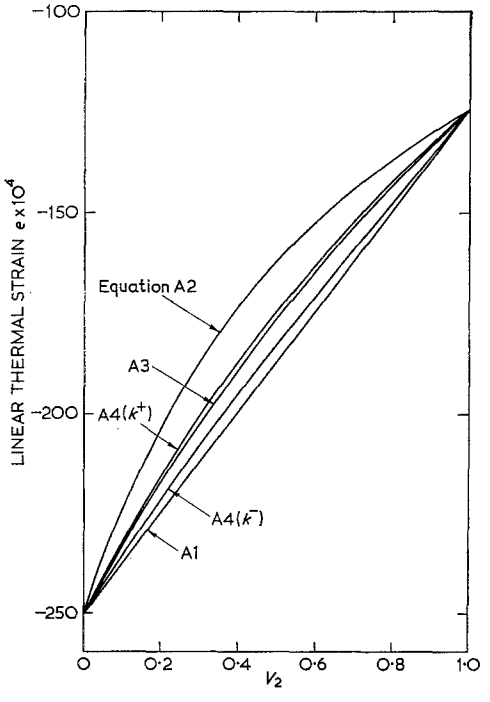

Figure 7 Linear thermal strain e of an isotropic, elastic, composite material, versus volume fraction of phase 2, v_2, according to various equations (with $e_1 = -250 \times 10^{-4}$, $e_2 = -125 \times 10^{-4}$, $\nu_1 = 0.4$, $\nu_2 = 0.3$ and $G_2 = 5G_1$).

Equation 17 to LPE comes from previous studies of other semicrystalline polymers which can be obtained in the wholly amorphous state. A corollary of Equation 17 is the equivalent relation between α and χ_v

$$\alpha = \chi_v \alpha_{cr} + (1 - \chi_v)\alpha_{am} . \qquad (18)$$

For specimens covering virtually the entire range of χ_v, Equation 18 (and, therefore, Equation 17) appears to hold for both poly 4-methyl 1-pentene [31] and polyethylene terephthalate [32]. That Equation 17 should apply to the present problem may be easily explained, at least for $T > T_g$, by the amorphous polymer flowing to relax thermal stresses.

Following Equation 17, at various temperatures T a straight line was constructed through the data points of $e(\chi_v)$, using the method of "least squares". These lines are shown for a selection of values of T in Fig. 8, together with the corresponding data points, cross-plotted versus χ_v from curves such as those of Fig. 6. This method yields both e_{am} and e_{cr} as functions of T. Results are plotted in Fig. 4, where the error bars correspond to standard error in e_{am}

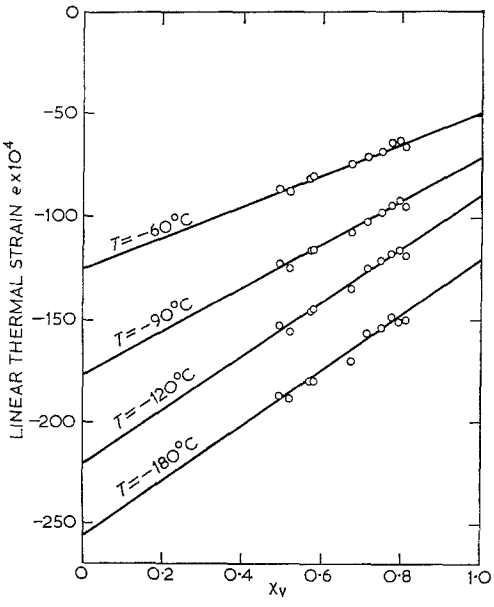

Figure 8 Linear thermal strain e of isotropic LPE plotted versus χ_v at various temperatures T, with "least squares" fitted straight lines.

and e_{cr} as obtained from the "least squares" fitting procedure. In addition the effective isotropic linear thermal strain of the crystal e_{cr} was calculated using the values of e_a, e_b and e_c obtained by Davis *et al* [6]. This is also shown in Fig. 4. There is good agreement between these X-ray values of e_{cr} and the values of e_{cr} obtained by the extrapolation procedure. This important result confirms that use of Equation 17 was entirely justified.

The results for $e_{am}(T)$ (Fig. 4) clearly show a change in gradient in the region of $T = -120°C$ corresponding to the γ-transition. From the present work, at the lowest temperatures considered $\alpha_{cr} = 0.45 \times 10^{-4} °C^{-1}$ and $\alpha_{am} = 0.42 \times 10^{-4} °C^{-1}$, supporting the findings of Fischer and Kloos [18] and Stehling and Mandelkern [5] that α is essentially independent of χ_v below the γ-relaxation temperature. Above the γ-transition also the present results are consistent with previous work. For $T = -105°C$, Fig. 4 yields $\alpha_{am} = 1.5 \times 10^{-4} °C^{-1}$, compared with $\alpha_{am} = 1.8 \times 10^{-4} °C^{-1}$ measured by Stehling and Mandelkern [5].

In the remainder of this paper, $e_{am}(T)$ as plotted in Fig. 4 will be assumed to be the linear thermal strain of amorphous LPE, as measured under the present experimental conditions for both isotropic and oriented specimens.

5. Discussion

5.1. Anisotropy of thermal expansion

It was pointed out above that the anisotropy of thermal strain in the oriented sample of LPE (Fig. 3) broadly corresponds to that in the LPE crystal, and that this is to be expected from the approximately single-crystal texture of the specimen. Is it possible, however, to predict more closely the anisotropy, taking into account a contribution to thermal expansion from the amorphous fraction?

A possible means of achieving this is provided by the model proposed by Takayanagi *et al* [2], for describing mechanical coupling between crystal and amorphous regions in oriented LPE. Similar models have been used successfully to explain thermal expansion data for other materials (e.g. graphite – see Slagle [33]).

Let the model of Fig. 9 apply for calculating e_x, e_y and e_z. This is the simplest form of the Takayanagi model as proposed for oriented LPE [2]. Crystal and amorphous phases are simply taken to be coupled linearly in series in the Z direction and in parallel in X and Y directions of the sheet. Making the approximations that all crystal c-axes are parallel to Z, all b-axes parallel to Y and all a-axes parallel to X, and assuming both phases to be elastic, affords the following equations for e_x, e_y and e_z:

$$e_x = \frac{\chi_v E_a e_a + (1 - \chi_v) E_{am} e_{am}}{\chi_v E_a + (1 - \chi_v) E_{am}} \quad (19a)$$

$$e_y = \frac{\chi_v E_b e_b + (1 - \chi_v) E_{am} e_{am}}{\chi_v E_b + (1 - \chi_v) E_{am}} \quad (19b)$$

$$e_z = \chi_v e_c + (1 - \chi_v) e_{am} \quad (19c)$$

where E_a and E_b are the tensile modulus of the LPE crystal in a and b directions and E_{am} the tensile modulus of amorphous LPE. χ_v takes its value at 0°C.

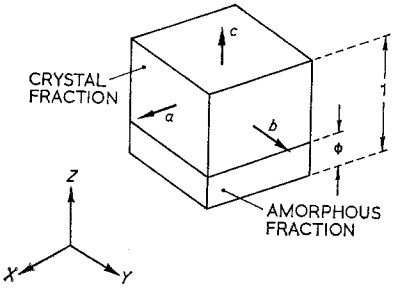

Figure 9 Model for calculating linear thermal strain of biaxially oriented specimen, where $\phi = 1 - \chi_v$.

In evaluating Equations 19a-c, e_{am} was assumed equal to that found by extrapolation in Section 4 from measurements on isotropic LPE (Fig. 4). For e_a, e_b and e_c, the data of Davis *et al* [6] (also plotted in Fig. 4) were used. Volume fraction crystallinity χ_v was taken to be 0.80, as determined from the density of the oriented sheet. The crystal tensile moduli E_a and E_b were equated to 6.81×10^{10} and 9.18×10^{10} dyn cm^{-2} respectively, as predicted theoretically by Odajima and Maeda [34] for − 196°C (values calculated from Set I of their paper). These moduli were assumed independent of temperature between − 196 and − 80°C. The tensile modulus $E_{am}{}^T$ of amorphous LPE at temperature T, was calculated from the dynamic shear modulus $G_{am}{}'^T$ (0.67 Hz) measured by Gray and McCrum [26], assuming a Poisson's ratio for amorphous LPE of 0.5 (independent of time and temperature). It should be noted that $E_{am}{}^T$ is also a function of time in the γ-relaxation region of temperature. We expect, therefore, Equations 19a and b to be exact in the relaxed and unrelaxed regions, but approximations at the centre of the relaxation. Another weakness of Equations 19a and b is that the phase moduli are assumed independent of strain up to tensile strains of ca. 0.025, at the lowest temperatures considered. This assumption is necessary since the strain dependence of these moduli at low temperatures is unknown.

Results of the calculation are compared with experimental data in Fig. 3. The error bars arise from quoted possible errors in e_{am}, e_a, e_b, e_c and $G_{am}{}'^T$ (0.67 Hz). It is clear that the overall pattern of anisotropy is correctly predicted. On a quantitative level, however, there is not good agreement. Furthermore, the disagreement cannot be explained simply by incomplete orientation of crystal axes. The most likely explanation for the lack of close agreement is that the model of linear coupling between the phases provides only a first approximation (albeit a reasonable one) to the behaviour of single-crystal texture of LPE, which in reality consists of stacks of alternating lamellar layers of crystal and amorphous polymer. The lamellar nature of crystal and amorphous regions (already known to dominate the mechanical anisotropy of oriented LPE at high temperatures [17, 35]) and interactions between adjacent stacks are not taken into account by the simple Takayanagi model. There is the further possibility that the values of e_a, e_b ,e_c and e_{am} obtained for isotropic

LPE are not identical to their counterparts in oriented LPE.

An unusual result from the calculations is the minimum predicted in e_z in the γ-relaxation region of temperature (see Fig. 3). This minimum is just discernible in the experimental measurements of e_z. It occurs because of the negative α_c (see above, Section 2) and the large increase in α_{am} in the γ-region.

Another interesting feature of the results is an inflection in the calculated $e_y(T)$ curved, also in the γ-region of temperature. This occurs because of the abrupt change in E_{am} which takes place in this temperature range. The inflection is not, however, discernible in experimental measurements of $e_y(T)$ (see Fig. 3).

In conclusion, moderate success has been achieved by comparing the predictions of the simple linear model with experimental thermal expansion results for single crystal texture LPE. The overall pattern of anisotropy has been correctly predicted, but differences remain on the quantitative level.

5.2. Thermal expansion of a spherulite

In this section, we attempt to understand the thermal expansion of a spherulite in terms of the thermal expansion of the single crystal texture specimen. The accepted model of a spherulitic element is outlined in Fig. 10 and is in good agreement with observation. The spherulite is formed of stacks of lamellar crystals with interspersed amorphous lamellae. The crystal b-axis lies along the spherulite radius. The lamellae are twisted around b so that the vectors a and c have no preferred orientation in the plane normal to the spherulite radius.

It will be seen that the element shown in Fig. 10 is very realistically modelled by the single-crystal texture specimen (Figs. 1 and 2). We, therefore, inquire into the effect of 1. attributing to the spherulitic element of Fig. 10 principal expansion coefficients equal to the principal expansion coefficients of the single crystal texture specimen; 2. the twist of the lamellae around the spherulite radius vector.

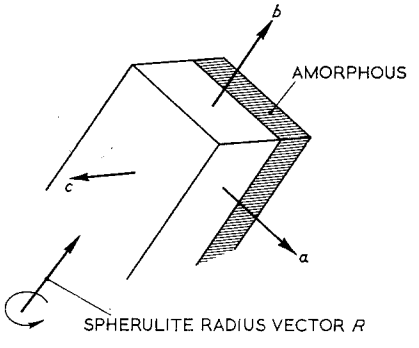

Figure 10 Model of an element of a spherulite showing a crystalline lamella and adjacent amorphous material. The lamellae are twisted around R as indicated.

In the discussion, we compare the single crystal texture specimen of crystallinity $\chi_v = 0.80$ with an equivalent isotropic specimen of the same crystallinity. From the measured volumetric thermal strain of the single-crystal texture specimen a linear thermal strain $\bar{e}$ was calculated using Equation 5. The linear thermal strain e(iso) of the equivalent isotropic specimen ($\chi_v = 0.80$) was calculated using for e_{cr} and e_{am} the values obtained by extrapolation and shown in Fig. 4. The quantities $\bar{e}$ and e(iso) are plotted in Fig. 11 and compared there with e_y.

Now if the single crystal texture specimen is a good model for the spherulitic element, then e_y must equal the principal thermal strain along the spherulite radius. The latter is equal to the overall linear thermal strain e(iso) of the spherulitic solid. It follows according to this argument, that e_y should equal e(iso). This is true to within 7% over the entire temperature range from $-$ 180 to 0°C (Fig. 11).

Over the temperature range $-$ 120 to 0°C it will be seen from Fig. 11 that e_y equals $\bar{e}$ to within 5%. From this it follows that not only does e_y lie between e_x and e_z (Fig. 3) but that the average of e_x and e_z equals e_y to within 5%. In the spherulite it is to be expected that the average of the principal thermal strains normal to the spherulite radius should equal the principal thermal strain along the radius. So in this respect also the single crystal texture specimen replicates correctly the thermal strain of the spherulitic element. The twist of the lamella is thus a significant morphological factor in lowering thermoelastic stresses within the spherulite.

5.3. Thermal stress in polyethylene

In polycrystalline metals with anisotropic thermal expansion (in the hexagonal metals zinc, cadmium and tin [36] and in the orthorhombic metal α-uranium [37, 38]), a change in temperature gives rise to stresses at those interfaces where two crystals of different orientations adjoin. These stresses have pronounced mechanical effects and cause plastic working of the solid, cracking [36] and an acceleration of creep rate [37, 38]. Analogous effects are observed in

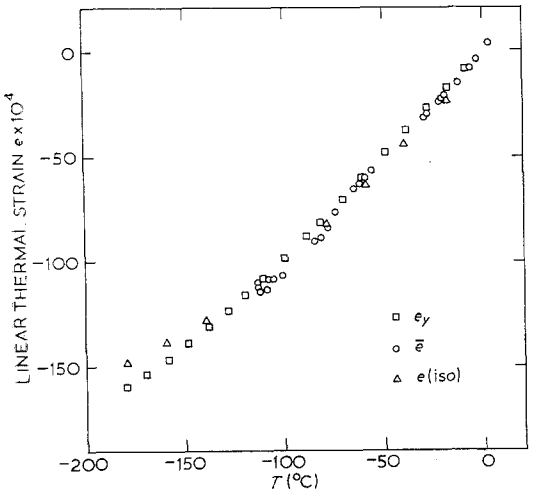

Figure 11 Temperature dependence of e_y for the oriented specimen compared with the mean value of linear thermal strain $\bar{e}$ for the same specimen and the linear thermal strain e(iso) for an isotropic specimen with crystal volume fraction $\chi_v = 0.80$ (equal to that of the oriented specimen).

isotropic LPE when the temperature is changed quickly [39, 40].

Thermal stress in LPE could be expected from two causes: 1. mismatch between the crystallographic orientation of adjacent crystals; 2. difference between thermal expansion of crystalline and amorphous LPE. Of these, 1. occurs because LPE is a polycrystalline aggregate and 2. because it is a two-phase material. Comparison of the linear thermal strain of the single-crystal texture specimen with that of the equivalent isotropic specimen enables these two effects to be separated because 1. will be absent in the single-crystal texture specimen.

The facts that $\bar{e} = e$(iso) and $e_y = e$(iso) show clearly that in isotropic spherulitic LPE hydrostatic thermal stresses from cause 1 (mismatch between adjacent crystals) are small. It could well be that the particular twisted habit of the crystal in the spherulite and the consequent averaging out of the vastly different thermal strains in the a and c directions minimizes thermal stresses due to cause 1. Another possibility is that stress relaxation processes in the amorphous fraction reduce the thermal stress to negligible proportions. This explanation is supported by the observation that polycrystalline n-paraffins cooled to liquid nitrogen temperature normally crack due to anisotropic thermal expansion [41].

In both single-crystal texture and isotropic LPE, however, thermal stresses will surely arise from cause 2. These will be mainly confined to acting in the plane of the lamellae. Furthermore, the present study shows that they act mostly in the b direction because of the large difference between e_{am} and e_b and the near equality between e_{am} and e_a (see Fig. 4). It is likely that stress relaxation processes will cause the thermal stress distribution to decay, particularly if the specimens are cooled slowly. These stresses are of the type termed tesselated stresses by Laszlo [42].

6. Summary and conclusions

Linear polyethylene, in spite of its complex microstructure, may be treated as a simple two-phase composite material for the purpose of explaining most of its macroscopic properties. This approach has already been successfully applied to low temperature mechanical properties of isotropic [26] and anisotropic LPE [2-4]. The present work shows that thermal expansion of both isotropic and anisotropic LPE can be sensibly rationalized within the same framework.

The simple "rule of mixtures" for thermal expansion, previously used without justification for semicrystalline polymers, when examined in the light of existing theories for composite materials appears to be an acceptable approximation for isotropic LPE. It is used to obtain by extrapolation the thermal expansion of amorphous LPE, e_{am}, over the temperature range from -190 to $+20°C$.

Thermal expansion of a single-crystal texture specimen of LPE, prepared with unique preferred orientation of each of crystal axes a, b and c, is highly anisotropic. The pattern of anisotropy follows in general features that of thermal expansion of the polyethylene crystal unit cell, as measured by X-ray diffraction. Fair agreement with experiment is obtained by allowing a contribution to thermal expansion from the amorphous fraction. For this purpose the single crystal texture specimen is represented by a simple model, in which crystal and amorphous regions are coupled in series in the draw direction and in parallel in both transverse directions.

When the single crystal texture specimen and an isotropic specimen of equal crystallinity are cooled in the range 0 to $-120°C$, the changes in volume are equal. This means that hydrostatic thermal stresses in the isotropic, spherulitic specimen due to the mismatch of adjacent crystals are essentially absent. This follows since

thermal stresses of this origin cannot occur in the single texture specimen. However, it is likely that thermal stresses due to the differences between thermal expansion coefficients of crystalline and amorphous polyethylene will occur in both single crystal texture and isotropic linear polyethylene.

It is shown that the single-crystal texture specimen is a good model from a textural point of view of an element of a spherulite. It is observed that for the single crystal texture specimen the mean of e_x and e_z equals e_y to within 5%. It follows that the twist of lamellae around a spherulite radius causes the principal thermal strain along the spherulite radius to be essentially equal to the mean of the two principal thermal strains normal to the spherulite radius. The twist of the lamellae is thus a significant morphological factor for reducing thermal stress in the spherulite.

Appendix

Thermal expansion of two-phase composite materials

Several theories have been proposed for calculating the linear thermal expansion coefficient α for isotropic, elastic, two-phase composite materials. We shall consider here only those theories which apply when both phases are isotropic, elastic and of arbitrary geometry. In order to aid comparison with experiment the various formulae will be rewritten in terms of the linear thermal strain e.

Let subscripts 1 and 2 refer to the respective phases and let v_i be the volume fraction of phase i. The simplest assumption to make is that no thermal stresses are set up when the temperature of the composite is changed. If this is so, we have

$$e = v_1 e_1 + v_2 e_2 \qquad \text{(A1)}$$

which is sometimes known as the "rule of mixtures". In practice, if $e_1 \neq e_2$ thermal stresses are set up within the composite and, therefore, Equation A1 is invalid. Other theories aim to correctly take thermal stresses into account.

Turner [43] assumed that the volumetric strains within each phase are constrained to be equal. Under these conditions

$$e = \frac{v_1 k_1 e_1 + v_2 k_2 e_2}{v_1 k_1 + v_2 k_2} \qquad \text{(A2)}$$

where k denotes a bulk modulus. Some agreement was obtained with data obtained for metal–metal composites [43].

Thomas [29] studied thermal expansion in polymers containing a series of inorganic fillers. Good agreement with results was obtained for an empirical relationship which, in terms of e, takes the form

$$\log e = v_1 \log e_1 + v_2 \log e_2 . \qquad \text{(A3)}$$

A series of theoretical studies [44-47] have shown independently that if the bulk modulus, k, of the composite is known, e may be given by

$$e = \bar{e} + \frac{(e_1 - e_2)}{\left(\frac{1}{k_1} - \frac{1}{k_2}\right)}\left[\frac{1}{k} - \left(\frac{\bar{1}}{k}\right)\right] \qquad \text{(A4)}$$

where $\bar{e} \equiv v_1 e_1 + v_2 e_2$ and

$$(\bar{1}/k) \equiv (v_1/k_1) + v_2/k_2) .$$

Often k is unknown, then bounds on e may be found from Equation A4, by using for k the upper and lower bounds derived by Hashin and Shtrikman [48] and Hill [49]:

$$k^- \leqslant k \leqslant k^+ \qquad \text{(A5)}$$

where

$$k^+ = k_2 + \frac{v_1}{1/(k_1 - k_2) + 3v_2/(3k_2 + 4G_2)}$$

and

$$k^- = k_1 + \frac{v_2}{1/(k_2 - k_1) + 3v_1/(3k_1 + 4G_1)}$$

given that $k_2 > k_1$ and $G_2 > G_1$.

References

1. W. J. DULMAGE and L. E. CONTOIS, *J. Polymer. Sci.* **28** (1958) 275.
2. M. TAKAYANAGI, K. IMADA, and T. KAJIYAMA, *ibid Part C* **15** (1966) 263.
3. C. P. BUCKLEY, R. W. GRAY, and N. G. MCCRUM, *ibid Part B* **7** (1969) 835.
4. *Idem, ibid* **8** (1970) 341.
5. F. C. STEHLING and L. MANDELKERN, *Macromol.* **3** (1970) 242.
6. G. T. DAVIS, R. K. EBY, and J. P. COLSON, *J. Appl. Phys.* **41** (1970) 4316.
7. C. W. BUNN and T. C. ALCOCK, *Trans. Faraday Soc.* **41** (1945) 317.
8. C. SELLA, *C.R. Acad. Sci. Paris* **248** (1959) 2348.
9. E. A. COLE and D. R. HOLMES, *J. Polymer Sci.* **46** (1960) 245.
10. M. TAKAYANAGI, T. ARAMAKI, M. YOSHINO, and K. HOASHI, *ibid* **46** (1960) 531.
11. J. H. WAKELIN, A. SUTHERLAND, and L. R. BECK, *ibid* **42** (1960) 278.
12. LI LI-SHEN, N. S. ANDREYEVA, and V. A. KARGIN, *Vysokomol. Soedin.* **3** (1961) 1238.
13. P. R. SWAN, *J. Polymer Sci.* **56** (1962) 403.
14. S. ZALWERT, *Makromol. Chem.* **131** (1970) 205.
15. Y. KOBAYASHI and A. KELLER, *Polymer* **11** (1970) 114.

16. S. M. OHLBERG and S. S. FENSTERMAKER, *J. Polymer Sci.* **32** (1958) 514.
17. C. P. BUCKLEY and N. G. MCCRUM, *J. Mater. Sci.* **8** (1973) 928.
18. E. W. FISCHER and F. KLOOS, *J. Polymer Sci. Part B* **8** (1970) 685.
19. F. DANUSSO, G. MORAGLIO, and G. TALAMINI, *ibid* **21** (1956) 139.
20. M. L. DANNIS, *J. Appl. Polymer Sci.* **1** (1959) 121.
21. M. G. GUBLER and A. J. KOVACS, *ibid* **34** (1959) 551.
22. K. TANAKA, *Bull. Chem. Soc. Japan* **33** (1960) 1060 and 1133.
23. R. NAKANE, *J. Appl. Polymer Sci.* **3** (1960) 124.
24. F. A. QUINN and L. MANDELKERN, *J. Amer. Chem. Soc.* **80** (1958) 3178.
25. E. W. FISCHER, H. GODDAR, and G. F. SCHMIDT, *J. Polymer Sci. Part A-2* **7** (1969) 37.
26. R. W. GRAY and N. G. MCCRUM, *ibid* **7** (1969) 1329.
27. R. CHIANG and P. J. FLORY, *J. Amer. Chem. Soc.* **83** (1961) 2857.
28. J. A. SAUER, A. E. WOODWARD, and N. FUSCHILLO, *J. Appl. Phys.* **30** (1959) 1488.
29. J. P. THOMAS, General Dynamics, Fort Worth, Texas, USA Report AD287826 (1960).
30. L. E. NIELSEN, *J. Comp. Mater.* **1** (1967) 100.
31. J. H. GRIFFITH and B. G. RÅNBY, *J. Polymer Sci.* **44** (1960) 369.
32. K. H. HELLWEGE, J. HENNIG, and W. KNAPPE, *Kolloid-Z.u.Z. Polymere* **186** (1962) 29.
33. O. D. SLAGLE, *Carbon* **6** (1968) 111.
34. A. ODAJIMA and T. MAEDA, *J. Polymer Sci. Part C* **15** (1966) 55.
35. G. R. DAVIES, A. J. OWEN, I. M. WARD, and V. B. GUPTA, *J. Macromol. Sci.-Phys. B* **6** (1972) 215.
36. W. BOAS and R. W. K. HONEYCOMBE, *Proc. Roy. Soc. A* **186** (1946) 57 and **188** (1947) 427.
37. G. W. GREENWOOD, *J. Inst. Metals* **88** (1959) 31.
38. W. S. BLACKBURN, G. HARNBY, and J. J. STABO, *J. Nucl. Energy A* **12** (1960) 162.
39. J. M. HUTCHINSON and N. G. MCCRUM, *Nature Phys. Sci.* **236** (1972) 115.
40. J. W. COOPER and N. G. MCCRUM, *J. Mater. Sci.* **7** (1972) 1221.
41. J. M. CRISSMAN and E. PASSAGLIA, *J. Appl. Phys.* **42** (1971) 4636.
42. F. LASZLO, *J. Iron Steel Inst.* (a) **147** (1943) 173; (b) **148** (1943) 137; (c) **150** (1944) 183; (d) **152** (1945) 207.
43. P. S. TURNER, *J. Res. N.B.S.* **37** (1946) 239.
44. V. M. LEVIN, *Inzh. Zh. Mekh. Tverd. Tela* **2** (1967) 88.
45. R. A. SCHAPERY, *J. Comp. Mater.* **2** (1968) 380.
46. J. L. CRIBB, *Nature* **220** (1968) 576.
47. B. W. ROSEN and Z. HASHIN, *Int. J. Engng. Sci.* **8** (1970) 157.
48. Z. HASIN and S. SHTRIKMAN, *J. Mech. Phys. Solids* **11** (1963) 127.
49. R. HILL, *ibid* **11** (1963) 357.

Received 13 November 1972 and accepted 5 February 1973.